Electro-optic Polymer Infiltrated Silicon Slot Photonic Crystal Waveguide for Broadband Electromagnetic Field Sensing

[1]Xingyu Zhang*, [2]Amir Hosseini, [2]Harish Subbaraman, [3]Shiyi Wang, [3]Qiwen Zhan, [4]Jingdong Luo, [4]Alex K.-Y. Jen, and [1]Ray T. Chen*

[1]*Microelectronics Research Center, Electrical and Computer Engineering Department, University of Texas at Austin, Austin, TX, 78758, USA*
[2]*Omega Optics, Inc., Austin, TX 78759, USA*
[3] *Department of Electrical and Computer Engineering, University of Dayton, Dayton, OH 45469, USA*
[4] *Department of Materials Science and Engineering, University of Washington, Seattle, Washington 98195, USA*
**Corresponding author: xzhang@utexas.edu, raychen@uts.cc.utexas.edu*

Abstract: We demonstrate an integrated photonic electromagnetic field sensor based on an electro-optic polymer infiltrated slot photonic crystal waveguide modulator. The minimum detectable electric field is measured to be 2.5V/m at 8.4GHz.

OCIS codes: (280.4788) Optical sensing and sensors; (130.5296) Photonic crystal waveguides; (130.4110) Modulators

Electromagnetic field (EMF) sensors have shown promising applications in high power microwave and electromagnetic pulse detection, process control, RF IC testing, and so on [1]. Traditional electronic EMF sensors have large conductive probes which perturb the field to be measured and also make the device bulky. To address these problems, integrated photonic EMF sensors have been developed, in which an optical signal is modulated by an RF signal collected by a small enough antenna [2]. Such photonic devices have a few inherent advantages over conventional electronic sensors, such as compact size, high sensitivity, broad bandwidth, and noise immunity. In this paper, we design and demonstrate a compact, sensitive and broadband integrated photonic EMF sensor based on a bowtie antenna coupled silicon-organic hybrid (SOH) slot photonic crystal waveguide (SPCW) modulator. Slow-light effects in the electro-optic (EO) polymer refilled silicon SPCW [3], together with the broadband electric field enhancement provided by the bowtie antenna, are utilized to enable an ultra large effective in-device EO coefficient (r_{33}) over 1000pm/V [4] and thus high sensitivity.

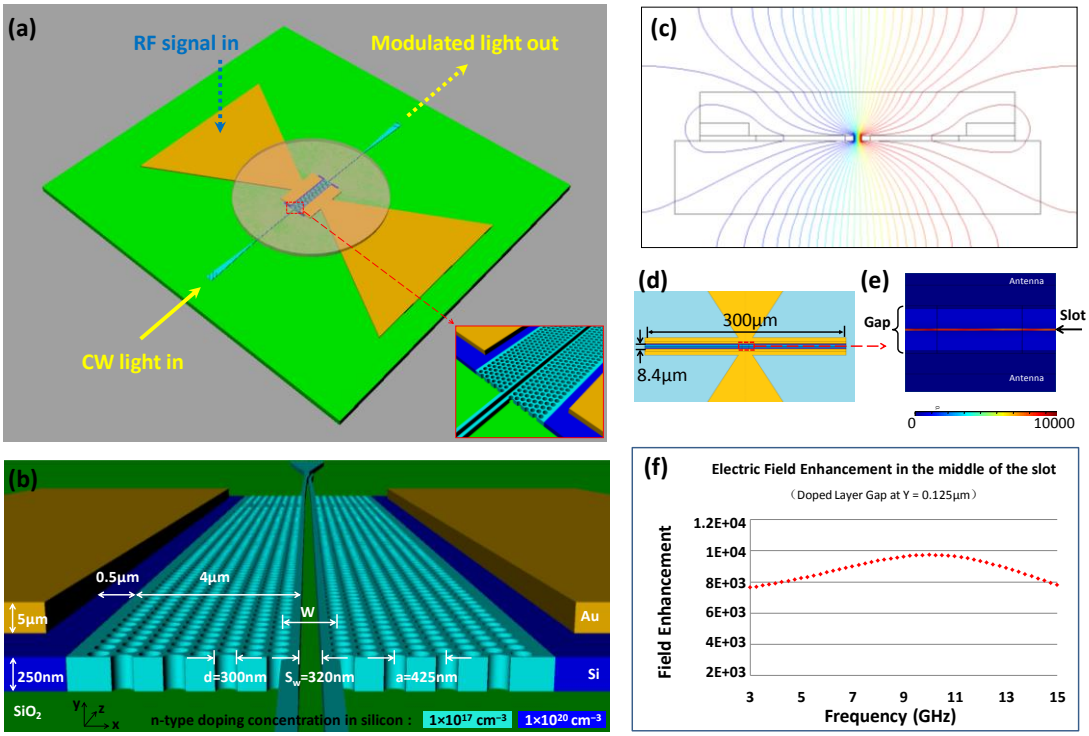

Fig. 1. (a) Schematic view of the key part of the electromagnetic field sensor consisting of an EO polymer refilled SPCW phase modulator and a bowtie antenna. An external arm is combined with this phase modulator to form a MZI structure, converting phase modulation to intensity modulation. (b) Tilted view showing the cross section of the antenna-coupled SPCW, with two-level n-type silicon doping. (c) Cross-sectional view of RF (10GHz) electric potential distribution across the doped silicon SPCW. (d) and (e) Enhanced electric field distribution inside the antenna feed gap. (f) Electric field enhancement factor inside the slot versus RF frequency.

The key part of our photonic EMF sensor consisting of an EO polymer refilled silicon slot PCW phase modulator coupled with a gold bowtie-shaped antenna is shown schematically in Fig. 1 (a). EO polymer SEO125 (r_{33}=125pm/V) is used to refill the 300μm-long silicon SPCW on SOI substrate. This EO polymer refilled silicon slot PCW with a slot

width (S_w) of 320nm is band-engineered by lateral shifting method to achieve low-dispersion slow-light propagation over a broad wavelength range of 8nm [4], as well as high optical mode confinement inside the EO polymer refilled slot. A strip- to slot-waveguide mode converter is designed to connect the device to the input and output strip waveguides [5]. The silicon slot PCW is embedded in the feed gap of the bowtie antenna with capacitive extension bars, as shown in Fig. 1 (a). The bowtie antenna is used as a receiving antenna, driving electrodes, and poling electrodes. With the two bowtie arms as receivers, a confined resonant electric field with strong enhancement factor can be generated in the feed gap. The working principle of our photonic EMF sensor is as follows. The bowtie antenna collects incident electric field, transforms it into high power density electric field within its feed gap, and directly modulates the phase of optical CW signal propagating along the EO polymer refilled SPCW embedded within the feed gap. For measurement, we convert this phase modulation to intensity modulation using an external arm enabled MZI structure. In this way, the amplitude of an incident EMF is characterized by measuring the intensity of the modulated optical signal.

In order for our sensor to operate in GHz regime, the top silicon layer is selectively ion implanted with P+ at the concentration of $1\times10^{17}cm^{-3}$ and $1\times10^{20}cm^{-3}$, as shown in Fig. 1 (b), to reduce the PCW resistivity and thus the RC time delay, while electric field inside the slot is also maximized [6]. Effective medium approximations [7] are to calculate effective silicon resistivity and effective silicon RF dielectric constant. Fig. 1 (c) shows the simulated cross-sectional view of the RF electric potential distribution ($1V_{AC}$, 10GHz) across the device, showing over 90% of voltage drops inside the slot. With bow arm length of 3mm and flare angle of 60º, the bowtie antenna has a central resonant frequency at 10GHz [8]. Figs. 1 (d) and (e) show the simulated electric field uniformly enhanced in the PCW slot. Fig. 1 (f) shows the simulated spectrum of field enhancement (FE), defined as resonant electric field divided by incident electric field. It can be seen that the electric field inside the slot is enhanced by a maximum factor of ~10,000 at 10GHz, with a 1-dB RF bandwidth over 9GHz.

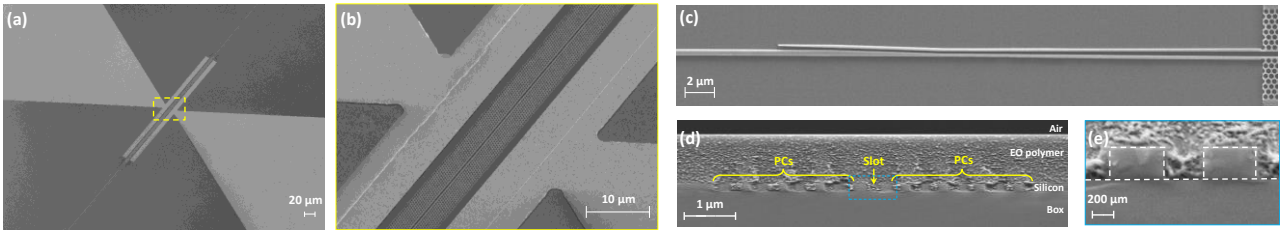

Fig. 2. (a) SEM image of the fabricated device. (b) Magnified SEM image of the yellow rectangular region in (a) shows the slot PCW region and bowtie antenna overlay. (c) SEM image of the new type mode converter for efficient coupling between strip waveguide to large-slot (320nm) PCW waveguide. (d) SEM image of cross section of the EO polymer refilled silicon slot PCW. PCs: photonic crystals. (e) Magnified SEM image of the blue rectangular area in (d).

The silicon photonic circuitries are fabricated using e-beam lithography, photolithography, RIE, and ion implantation, while a 5μm-thick gold bowtie antenna is patterned by photolithography and electroplating [9]. Some SEM images of fabricated device are shown in Figs. 2 (a)-(c). The inner sides of the extension bars of the bowtie antenna are connected to the silicon rails which are heavily doped for ohmic contact between the antenna and the PCW, as shown in Fig. 2 (b). Next, the EO polymer is infiltrated into the slot and holes of silicon PCW region by spincoating, as shown in Figs. 2 (d) and (e). Then the device is poled at an electric field of 100V/μm at 145 ℃ [10], in which the bowtie antenna serves as poling electrodes. In this process, the monitored leakage current density remains below $1.4\times10^{-6}A/m^2$ which is comparable to that measured in a thin film configuration ($2.36\times10^{-6}A/m^2$ in data sheet) [4], indicating that the 320nm-wide slot dramatically reduces leakage current through silicon/polymer interface compared to a sub-100nm slot [11].

After the device is fabricated, first, the bowtie antenna is tested to demonstrate its GHz broadband characteristic. A network analyzer is used to measure the S_{11} parameter (reflection signal) of the bowtie antenna. Assuming negligible loss, the transmission signal is inferred from the measured S_{11} as shown in Fig. 3 (a), from which a broadband response can be clearly seen. The peak response at 10GHz agrees well with the simulated peak resonance at 10GHz in Fig. 1 (f). This result indicates that our sensor can be used to detect the EMF over a broad frequency bandwidth in GHz regime.

Next, an EO modulation experiment is performed. An MZI system is formed using a 90/10 polarization maintaining fiber splitter, a 50/50 polarization maintaining fiber combiner and a variable optical attenuator (VOA), as shown in Fig. 3 (b). Our device is inserted in one arm as a phase modulator, and the VOA is on the other arm. 1556nm TE-polarized light is coupled to the MZI system. The VOA is adjusted until the optical power at the output of the external arm is equal to that coming out of the device. When the two beams from the two arms are combined at the output of this MZI system, the phase modulation is converted into intensity modulation. A sinusoidal RF signal with V_{pp}=1V at 100KHz is directly applied across the two bows, in which the bowtie antenna works as driving electrodes. Modulated optical output is collected by a photodetector and measured by a microwave spectrum analyzer (MSA). The measured response signal in Fig. 3 (c) indicates that the optical signal is modulated at the same frequency as the input RF signal. In addition, the modulation transfer function is also measured by a logic analyzer as shown in Fig. 3 (d), using a method similar to that used in [10, 12]. This low-frequency EO modulation experiment demonstrates the successful poling of EO polymer and the functionality of MZI which is then used in the next EMF sensing experiment.

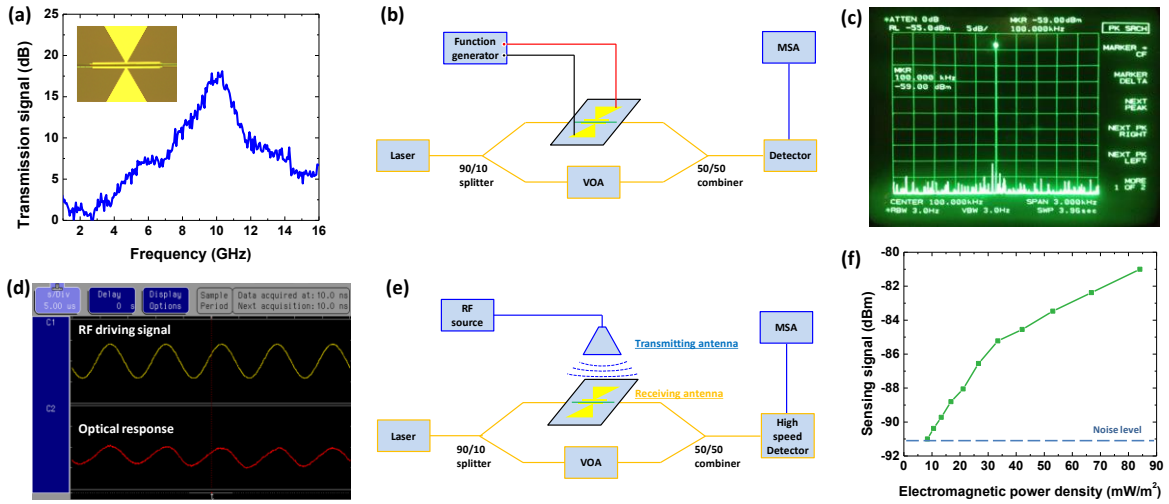

Fig. 3. (a) Measured S21 parameter of the broadband bowtie antenna. The inset shows a top-view microscope image of the fabricated device. (b) The schematic of the system for EO modulation experiment. (c) The EO modulation response signal as measured on the MSA. (d) EO modulation transfer function. (e) The schematic of the system for electromagnetic field sensing experiment. (f) The measured sensing signal as a function of electromagnetic power density at 8.4GHz.

To evaluate the EMF sensor, a sensing experiment is performed. The schematic of the experiment system is shown in Fig. 3 (e). An RF signal at 8.4GHz from a sweep oscillator is fed into a horn antenna (Gain G_t=6dB). The horn antenna is placed at R=30cm vertical distance above the sensor, which is beyond the far-field distance of the horn antenna so that electromagnetic waves can be treated as plane waves. The horn antenna works as a transmitting antenna and the bowtie antenna on the sensor works as a receiving antenna. A high-speed photodetector is used to detect the modulated signal at high frequency. The sensing signal is measured by the MSA. To characterize the sensitivity of this sensor to the electromagnetic power, the RF power applied on the horn antenna (P_t) is tuned, corresponding to the variation of EMF power density near the sensor based on Eq. 1.

$$S_{avg} = G_t P / 4\pi R^2 \quad (1)$$

where S_{avg} is the average Poynting vector. The measured sensing signal v.s. EMF power density is plotted in Fig. 3 (f). When the EMF power density decreases to 8.4mW/m^2, the sensing signal is below noise level. Based on Eq. 2, this minimum detectable EMF power density is used to estimate the minimum detectable electric field as 2.5V/m at 8.4GHz, considering the EMF has a predominantly plane-wave character within the far-field region of horn antenna. Details can be seen in ref [13].

$$|E| = \sqrt{2S_{avg} / \varepsilon_o \varepsilon_r c} = 2.5\text{V/m} \quad (2)$$

Reference

[1] C.-Y. Lin, A. X. Wang, B. S. Lee, X. Zhang, and R. T. Chen, "High dynamic range electric field sensor for electromagnetic pulse detection," *Opt. Exp*, vol. 19, pp. 17372-17377, 2011.

[2] V. Passaro, F. Dell'Olio, and F. De Leonardis, "Electromagnetic field photonic sensors," *Progress in quantum electronics*, vol. 30, pp. 45-73, 2006.

[3] X. Zhang, A. Hosseini, X. Lin, H. Subbaraman, and R. T. Chen, "Polymer-based Hybrid Integrated Photonic Devices for Silicon On-chip Modulation and Board-level Optical Interconnects," IEEE Journal of Selected Topics in Quantum Electronics, vol.19, no.6, pp.3401115, 2013

[4] X. Zhang, A. Hosseini, S. Chakravarty, J. Luo, A. K.-Y. Jen, and R. T. Chen, "Wide optical spectrum range, subvolt, compact modulator based on an electro-optic polymer refilled silicon slot photonic crystal waveguide," *Optics letters*, vol. 38, pp. 4931-4934, 2013.

[5] X. Zhang, H. Subbaraman, A. Hosseini, and R. T. Chen, "Optimization of Highly Efficient Mode Converter for Coupling Light into Wide slot Photonic Crystal Waveguide," (Under review)

[6] X. Zhang, A. Hosseini, X. Xu, S. Wang, Q. Zhan, Y. Zou, S. Chakravarty, and R. T. Chen, "Electric field sensor based on electro-optic polymer refilled silicon slot photonic crystal waveguide coupled with bowtie antenna," in *SPIE OPTO*, 2013, pp. 862418-862418-8.

[7] W. Perrins, D. McKenzie, and R. McPhedran, "Transport properties of regular arrays of cylinders," *Proceedings of the Royal Society of London. A. Mathematical and Physical Sciences*, vol. 369, pp. 207-225, 1979.

[8] X. Zhang, S. Wang, H. Subbaraman, Q. Zhan, and R. Chen, "Integrated broadband bowtie antenna on transparent substrate," (In preparation)

[9] X. Zhang, B. Lee, C.-y. Lin, A. X. Wang, A. Hosseini, and R. T. Chen, "Highly Linear Broadband Optical Modulator Based on Electro-Optic Polymer," *Photonics Journal, IEEE*, vol. 4, pp. 2214-2228, 2012.

[10] X. Lin, T. Ling, H. Subbaraman, X. Zhang, K. Byun, L. J. Guo, and R. T. Chen, "Ultraviolet imprinting and aligned ink-jet printing for multilayer patterning of electro-optic polymer modulators," *Optics letters*, vol. 38, pp. 1597-1599, 2013.

[11] X. Wang, C. Y. Lin, S. Chakravarty, J. Luo, A. K. Y. Jen, and R. T. Chen, "Effective in-device r< sub> 33</sub> of 735 pm/V on electro-optic polymer infiltrated silicon photonic crystal slot waveguides," *Optics Letters*, vol. 36, pp. 882-884, 2011.

[12] X. Zhang, A. Hosseini, C.-y. Lin, J. Luo, A. K. Jen, and R. T. Chen, "Demonstration of Effective In-device r33 over 1000 pmV in Electro-optic Polymer Refilled Silicon Slot Photonic Crystal Waveguide Modulator," in *CLEO: Science and Innovations*, 2013.

[13] X. Zhang, A. Hosseini, H. Subbaraman, S. Wang, Q. Zhan, J. Luo, A. Jen, R. Chen, "Integrated Photonic Electromagnetic Field Sensor Based on Broadband Bowtie Antenna Coupled Silicon Organic Hybrid Modulator", Journal of Lightwave Technology (Accepted).